

**ROCK TEXTURES AND GRAIN SIZES IN THE GLEN TORRIDON REGION (GALE CRATER, MARS) OBSERVED BY THE MARS HAND LENS IMAGER (MAHLI) AND CHEMCAM.** M.E. Minitti<sup>1</sup>, F. Rivera-Hernández,<sup>2</sup> K.A. Bennett<sup>3</sup>, S. Gupta<sup>4</sup>, and R.C. Wiens<sup>5</sup>. <sup>1</sup>Framework (Silver Spring, MD; minitti@me.com); <sup>2</sup>School of Earth and Atmospheric Sciences, Georgia Institute of Technology, Atlanta, GA; <sup>3</sup>USGS Astrogeology Science Center, Flagstaff, AZ; <sup>4</sup>Imperial College, London, UK; <sup>5</sup>Los Alamos National Laboratory, Los Alamos, NM.

**Introduction:** The Mars Science Laboratory (MSL) *Curiosity* rover began exploration of the “Glen Torridon” region of Gale crater on Sol 2299. The Glen Torridon (GT) region largely coincides with a trough exhibiting the spectral signature of smectite clays detected by CRISM [1,2]. Multiple drilled samples within GT have confirmed the presence of clays [e.g., 3]. Observations across the traverse through GT have defined at least two members within GT: the Jura and Knockfarril Hill (KHm) members [4]. The weathering characteristics of these two members are highly contrasting. The former forms surface exposures comprising a mix of granule- to very coarse-sized (~2-50 mm) pebbles and patches of coherent bedrock. The latter is characterized by coherent bedrock that in places exhibits cross bedding [4].

Between Sols 2299 and 2564, the Mars Hand Lens Imager (MAHLI) observed 80 targets within the Jura and KHm members at scales ranging from 20-40  $\mu\text{m}/\text{pixel}$  to assess texture and grain size, and ~50-150  $\mu\text{m}/\text{pixel}$  to assess bedrock structure. Where possible, dust and coatings were removed from targets using the Dust Removal Tool or the ChemCam laser. Targets were most commonly imaged from ~7 cm working distance (~30  $\mu\text{m}/\text{pixel}$ ) to support APXS analyses [e.g., 5]. These images provide a consistent scale to compare rock characteristics such as sedimentary textures (e.g., grain size and shape) and structures (e.g., planar lamination, cross-bedding), and superficial textures (e.g., color, weathering style).

Over the same interval, ChemCam analyzed 134 rock targets in the Jura and KHm members, typically employing 9 or 10 point rasters to support chemical analyses of the targets and grain size estimates using the Gini index mean score (GIMS) technique [6]. The GIMS technique is a grain-size proxy that quantifies point-to-point chemical variability in ChemCam laser induced breakdown spectroscopy data [6]. Twenty-four targets were analyzed by both MAHLI and ChemCam, supporting direct comparison of texture and grain size observations. The combined observations illuminate relationships between texture, and grain size in the Jura and KHm members within GT [4].

**MAHLI-defined texture classes:** Observations of MAHLI targets can be divided into five major texture classes, with some having overlapping characteristics. Most classes have red or gray rock exposures, but many

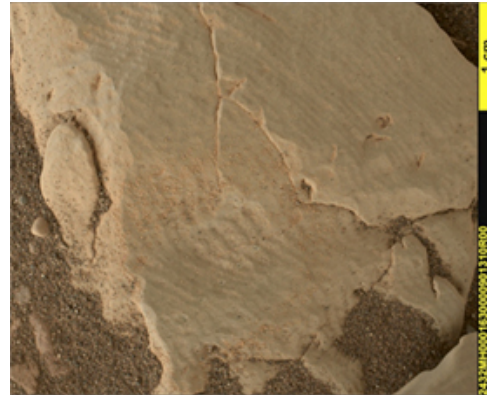


**Fig. 1:** Laminated clast (Gullane). This image (and all images) processed by D.M. Fey.



**Fig. 2:** Laminated/layered bedrock (Mons Graupius). Scale the same as the other figures.

targets within each class exhibit a combination of red and gray color.

**Laminated clasts.** Laminated clasts exist in a range of sizes (~2-50 mm), exhibit very thin (~200-400  $\mu\text{m}$ ), regular laminations, and are pitted (Fig. 1). Some clasts are tabular in form with internal laminations paralleling the face on which the clast rests on the surface, while other clasts are rounded to sub-angular with internal laminations cutting through the clast with no relationship to the clast orientation on the surface.

**Laminated bedrock.** Bedrock of this class has regular laminations on the same scale as the laminated pebbles (~150-450  $\mu\text{m}$ ). While each occurrence of this class is laminated, subsets are defined by other identifying characteristics. One subset has elongated, lamination-parallel pits. Another subset includes horizons with

laminations so fine that the horizons appear smooth and massive from a distance. In other occurrences of the laminated class, resolvable ( $\sim 100\text{--}150\ \mu\text{m}$ , very fine to fine sand) black and/or white grains are present. The color differences among the grains likely correspond to differing compositions. This subset is sometimes associated with bedrock that appears to be cross-stratified in Mastcam images.

*Alternating thin and thick laminated bedrock.* Some outcrop expressions of laminated bedrock are found interbedded with horizons that have generally thicker ( $\sim 500\ \mu\text{m}$  – 1 mm) layers. In many of these outcrops, the horizons with thin laminations repeatedly alternate with the horizons of thicker layers (Fig. 2). Other outcrop examples are dominated by thicker layers. Thicker layer horizons have rougher surfaces that collect modern windblown sand. Higher resolution imaging ( $<30\ \mu\text{m}/\text{pixel}$ ) of the thicker layers, reveals that some of them contain laminations of similar scales to the laminated horizons. Thus, it is possible that the whole outcrop is laminated uniformly throughout, but differences in cementing/diagenesis between the horizons lead to differences in erosional expression. This class is similar to Flodigarry type rocks identified at the same elevations in GT and Vera Rubin ridge (VRR) [4].



Fig. 3: Polygonally fractured bedrock (Crieff).

*Polygonally-fractured bedrock.* This class is characterized by layered bedrock with fractures dividing each layer into  $\sim 0.5\text{--}2\ \text{cm}$  angular segments (Fig. 3). Individual layers have smooth (mm to sub-mm scale surface roughness) texture and sometimes are also laminated. Measuring lamination or layer thickness in this class is challenged by the fact that most targets were viewed normal to layering.

*Rock Hall-like.* This class is characterized by knobby, pitted outcrops and clasts with greasy luster. Outcrops of this class also tend to be small, on the order of tens of cm across. Laminations are observed in some

areas of the targets, but cannot be traced for more than  $\sim 1\ \text{cm}$  due to the rough, knobby nature of the targets. These outcrops resemble the red Jura member of the VRR, in particular the drill target Rock Hall [e.g., 7].

**ChemCam-based grain sizes estimates:** Grain size estimates for 134 GT rocks provided by the GIMS technique indicate that  $\sim 80\%$  of GT rocks have mud-sized grains. The mud grain size range in GIMS data was calibrated using lab and image data from targets with grain sizes  $<62.5\ \mu\text{m}$  [6]. Coarser-grained (coarse silt through coarse sand) GT rocks were also detected at discrete intervals, in both the Jura and KHM members, suggesting the presence of sandstones. The dominant mud grain size estimate for GT rocks is consistent with the clay detected in GT drilled samples [e.g., 3].

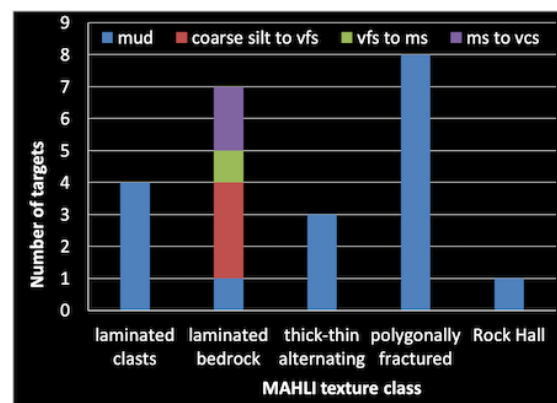


Fig. 4: Distribution of GIMS-determined grain sizes (colors in legend correspond to grain size categories) across MAHLI-defined texture classes.

**Relationship between texture classes and grain size:** Among the MAHLI-defined rock classes for GT, the majority of targets have mud grain sizes regardless of class (Fig. 4). However, the laminated bedrock class, with its internal variability, exhibits a range of grain sizes, from mud to very coarse sand. The variability of grain size among laminated bedrock targets is independent of whether targets are found within the Jura or KHM members or if they exhibit resolvable grains. Future work will seek to define sedimentary facies based on our collective observations.

**References:** [1] Milliken, R.E. et al. (2010) GRL, <https://doi.org/10.1029/2009GL041870>. [2] Fox, V.K. et al. (2019) LPSC 50, Abstract #2826. [3] Thorpe, M.T. et al. (2020) LPSC 51, Abstract #1524. [4] Fedo, C.M. et al. (2020) LPSC 51, Abstract #2345. [5] Thompson, L.M. et al. (2019) 9<sup>th</sup> Mars, Abstract #6304. [6] Rivera-Hernández, F. et al. (2019) Icarus, doi:10.1016/j.icarus.2018.10.023. [7] Horgan, B. et al. (2019) LPSC 50, Abstract #1424.